nzsee
NEW ZEALAND SOCIETY FOR EARTHQUAKE ENGINEERING

Panel zone strength in moment frames with slabs

C.P. Henderson, E.A. Macalister, G.A. MacRae & M. Bashiri
University of Canterbury, Christchurch, New Zealand.

ABSTRACT

Despite the common occurrence of composite slabs in steel structures, they are often excluded from design considerations, which may lead to undesirable panel zone yielding due to increased demands. Through the utilisation of finite element analyses of beam-column-slab-joint subassemblies, this study models the significance of slab effects on panel zone behaviour. The existing capacity design approach for the panel zone used in the New Zealand Steel Structures Standard (NZS 3404) is assessed. The analysis proved that the presence of a slab increased both the demand on, as well as the capacity of, the panel zone. Specifically, the capacity increase was observed to be 20% for the subassembly tested due to a change in yield mechanism caused by the slab. While results from the current NZS 3404 design method appear reasonable for the case considered, the background and concept was not clear, and it was based on only one analysis. A modified design method is proposed that clearly accounts for slab effects on the panel zone demand and capacity separately.

INTRODUCTION

In steel moment-resisting frame (MRF) structures, concrete floor slabs composite with the beam, in addition to providing flat level for building activities, increase the beam strength, allow lower interstorey heights, provide more economical construction, and improve the acoustic and fire performance. However, when the floor slab is in contact with the columns, bearing forces may result during large frame inelastic deformations increasing column demands. Since standards in most countries aim to encourage MRF beam sidesway mechanisms, with yielding concentrated at the beam ends and column bases, the increase in column demands needs to be quantified.

The New Zealand Steel Structures Standard (NZS 3404, 2007) considers slab interaction with the column by enhancing beam overstrength moments to determine design moments for the column itself, and for the column panel zone (PZ) (MacRae et al. 2007; Standards New Zealand 2007). The design approach increases PZ demands by half the amount that demands are increased for the column. This PZ design approach is not justified clearly and is based upon only one finite element analysis (Mago and Clifton 2008).

There is a need for designers to have simple, clear, and accurate design methods to discourage the PZ from becoming the major seismic energy-dissipating mechanism in the presence of a floor slab.

This paper seeks to address this need by seeking answers to the following questions:

1. How does PZ demand change with slabs and different subassembly configurations?
2. How does PZ capacity change with slabs and different subassembly configurations?
3. Are current NZS 3404 provisions reasonably predicting the required PZ capacity increase for design given slab effects?
4. What design recommendations can be made?

1 LITERATURE

1.1 Current Code Methods

Section 12 of the NZ steel standard general method (NZS 3404, 2007) uses the following approach to estimate the effect of the slab on the column moment. It firstly proposes that the compressive force developed between the slab and column, N_{slab}, is given by Equation 1 where b_{sef} is the width of slab in compression against the supporting column, taken as the breadth of the column flange, t_{ef} is the thickness of the concrete in contact with the column, A_g is the gross area of the beam framing into the column; and f_y is the beam flange yield strength (MacRae et al. 2007). It considers that the slab concrete strength increase over time is 10MPa greater than the 28 day concrete compressive strength, f'_c. The slab force is only assumed to be applied to the outside of the column as shown in Figure 1. This is known as Eurocode 8 Mode 1 as shown in Figure 2. Effects of other modes, Eurocode 8 Mode 2 and Mode 3, have been shown to be insignificant for most cases (Chaudhari et al. 2022; Alizadeh et al., 2018).

$$N_{slab} = min\left\{1.3t_{ef}b_{sef}(f'_c + 10MPa);\ \sum(A_g f_y)_i\right\} \quad (1)$$

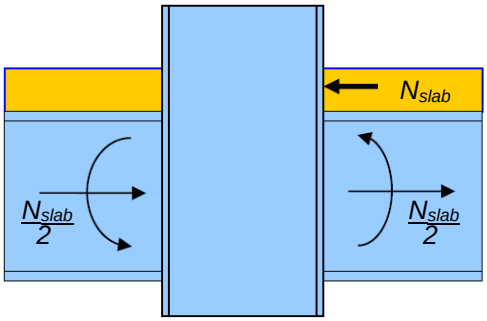

Figure 1. *Joint Horizontal Forces*

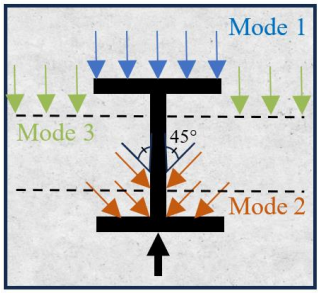

Figure 2. *Eurocode 8 slab force transfer mechanisms*

The beam moment-axial force interaction diagram is assumed to be given by Equation 2 (NZS1170.5). It indicates that the moments in the beams framing into the joint, ΣM_i^o, are reduced from their overstrength moment, $M_{b,i}^o$, given as the product of the overstrength factor (ϕ_{oms}) and section moment capacity (M_s), by the slab axial force, N_{slab}.

$$\Sigma M_i^o = min\left\{1.18\left(1 - \frac{N_{slab}}{\Sigma A_g f_{y,i}}\right)\Sigma M_{b,i}^o;\ \sum M_{b,i}^o\right\} \quad (2)$$

The design moment, M^o, for the column with composite beams framing into either side, before any dynamic effects are considered, is determined by taking moments about the beam centreline according to Equation 3 and Figure 1, where d_b is the steel beam depth, t_{eff} is the thickness of concrete in contact with the column, and t_o is the overall slab thickness.

$$M^o = \sum M_i^o + N_{slab}\left(\frac{d_b}{2} + t_o - \frac{t_{ef}}{2}\right) \quad (3)$$

A simplification of the NZS 3404 approach above, which is relevant for members of realistic size, gives the column design moment demand from beams, M^o, with concrete slabs in Equation 4 where ϕ_{omss} is an enhanced overstrength factor due to the slab effect which is given by Equation 5 (MacRae et al. 2007).

$$M^o = \phi_{omss} M_s \tag{4}$$

$$\phi_{omss} = \phi_{oms}\left(1 + 1.08\frac{t_{ef}}{d_b}\right) \tag{5}$$

For design of the panel zone (PZ), the enhanced overstrength factor in Equation 6 is used in NZS3404 (2007). Here, C_2 is a reduced version of the overstrength factor, ϕ_{oms}, which allows the PZ to yield before the column. This permits limited PZ yielding following Skiadopoulos et al. (2021). Omitting this nuance, the PZ demand increase due to a concrete slab is one half of that than the column. This assumption was justified by from one finite element analysis observing that the slab can increase the PZ strength as well as the PZ demand (Mago and Clifton, 2008).

$$\phi_{omss} = C_2\left(1 + 0.54\frac{t_{ef}}{d_b}\right) \tag{6}$$

1.2 Previous Research

MacRae and Gunasekaran (2007) proposed a simple concept for considering the effect of slab in moment frame buildings which calibrated well to the behaviour of reinforced concrete members. It considers that the slab wraps around the column and provides contact only on the compression face. Chaudhari et al. (2022) further developed this approach developing a hand method to estimate the likely performance which could be suitable for design. This was supported by more advanced numerical analyses and large scale test results. Experiments focused on the effects of slabs cast up to, as well as separated from, the column. He demonstrated that considering only the Eurocode 8 Mode 1 force transfer to the column was reasonable for typical situations because Mode 2 is generally activated only after concrete slab spalling has occurred in Mode 1. However, if the slab is well confined due to special detailing, then Modes 1 and 2 can act together significantly increasing the column demands. This needs to be considered in design, but it is not discussed in NZS3404 because it is not a common construction scenario. Alternatively, isolated slabs were also found to eliminate all slab damage and provide no increase in column demands, comparable to equivalent subassemblies without slabs. A separate study into the effects of Mode 3 concluded that for frames with un-isolated slabs, Mode 3 effects are negligible (Alizadeh et al. 2018).

1.3 Analytical Methods

Current NZS 3404 methods for determining the nominal shear capacity of the PZ utilise plastic mechanism analyses first introduced by Krawinkler (1978). The strength of the PZ for frames without slabs can be computed by considering the shear resistance of the column web and the bending resistance of the column flanges using energy methods, as shown in Figure 3. Secondary hinges may also occur in the beam flanges to form a full mechanism but due to moment-axial (M-P) interactions, these have low moment resistance and are generally ignored. NZS 3404 estimates the PZ capacity (V_{PZ}) using Equation 7 where t_{wc} is the column web thickness, t_p is the web doubler plate thickness, f_{yp}^* is the averaged yield strength of the web and doubler plate, d_b is the beam depth, d_c is the column depth, η considers column PZ axial-shear interaction, t_{fc} if the column flange thickness, and b_c is the column breadth.

$$V_{pz} = 0.6 f_{yp}^* d_c (t_{wc} + t_p)\eta\left[1 + \frac{3 b_c t_{fc}^2}{d_b d_c (t_{wc} + t_p)}\right] \tag{7}$$

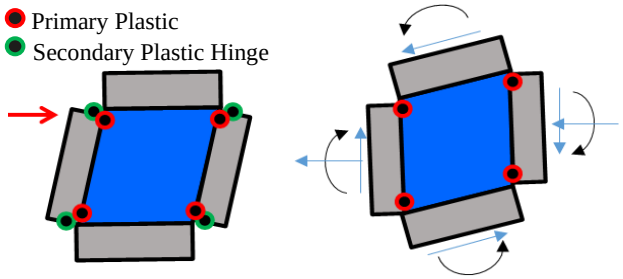

a) *Simple Mechanism* ***b)*** *Free Body*

Figure 3*. Bare steel frame plastic mechanism.*

2 METHODOLOGY

2.1 Reference Model Configuration

Beam-column-slab subassemblies were developed using ABAQUS (2022) finite element software to obtain the panel zone demands and capacities for a joint in a moment frame structure as shown in Figure 4 (Simulia 2022). To obtain validation, bare steel frame (BSF) and full depth slab (FDS) models from Chaudhari's thesis were initially adopted. Peak strength results were compared to Chaudhari's original results, with variations of less than 0.5% found. Minor discrepancies were attributed to difficulty upgrading software versions and changes to contact modelling techniques which are discussed below.

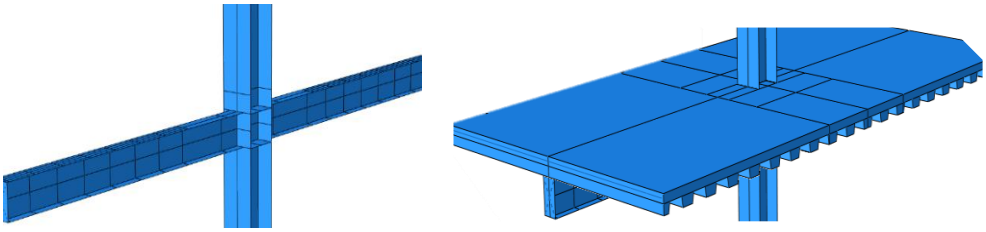

a) *Bare Steel Frame (BSF)* ***b)*** *Full Depth Slab (FDS)*

Figure 4. *Model Subassemblies.*

Table 1 presents all significant subassembly components, selected element types and associated member sizes. Shell elements were chosen for the steel frame and decking components to simplify the model, reduce computational demands, and reduce meshing difficulties compared to using solid elements.

The concrete slab was represented using a solid element to ensure precise interaction and to capture inelastic behaviour. Nonlinear springs were employed to replicate the effects of shear studs along the metal deck-to-beam interface, eliminating the need for additional solid elements. Following NZS 3404, no shear springs/studs were positioned within 1.5 times the beam depth from the column face. The subassembly measured 6m wide, 3m deep, and 2.1m high.

Gusset plates used in Chaudhari's steel frame models were excluded from these analyses. This was done for simplicity and because many fabricators now recommend using thicker end plates instead of gusset plates to reduce connection costs (Carson 2023).

While consistent with Chaudhari's analyses, other significant modelling decisions included (i) providing full bond (no slip) between the concrete slab, (ii) and fully bonding the rebar mesh and concrete slab, and merging the steel members to simulate stiff, welded connections as fixed connections would be critical, giving worst-case PZ demands.

***Table 1**. Description of reference model elements.*

Member	Element Type	Size
Beam (Both Sides)	S4R 'Shell'	310 UB 32
Column	S4R 'Shell'	310 UC 158
PZ Doubler Plate(s)	S4R 'Shell'	2 x 16 mm thick
Continuity Plates	S4R 'Shell'	16 mm thick
Beam Stiffener Plates	S4R 'Shell'	8 mm thick
Slab	C3D8R 'Solid'	150 mm deep
Reinforcing (Rebar) Mesh	B31R 'Two node beam'	8mm bar 200 x 200 mm grid
Steel Decking	S4R 'Shell'	ComFlor 80
Shear Studs	Spring Element 1-D	Two rows, 300 mm spacing

2.2 Boundary Conditions and Contact

Model boundary conditions are illustrated in Figure 5. The beam ends had ‘roller-like’ supports (z-displacement and x-rotation allowed), while the column base was ‘pinned’ (x-rotation allowed). Out-of-plane restraint was provided at all member ends. This was achieved by joining all surface nodes with wire elements and assigning tie constraints, creating one central master node. Boundary conditions were then applied to only the master node.

Given software improvements, contact was modelled utilising the ABAQUS general contact feature, and contact pairs were assigned to relevant regions of the column, slab, metal deck, and beam flange. This differed from the original models that used the surface-to-surface contact feature. Ingress was explicitly prevented between bearing elements, and a friction coefficient of 0.2 was applied to sliding components.

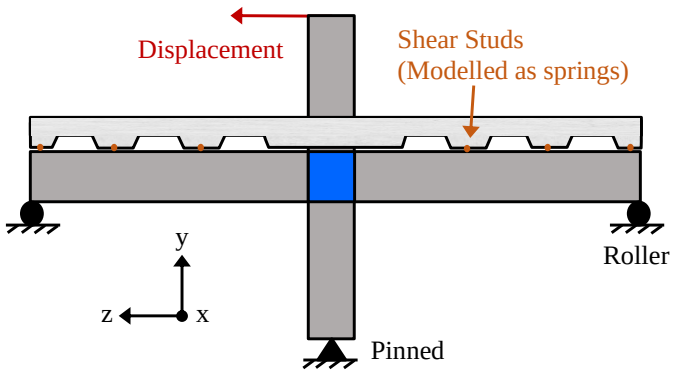

***Figure 5.** Idealised model boundary conditions.*

2.3 Panel Zone Considerations

2.3.1 Demand Assessment

To check the accuracy of current NZS 3404 methods, the influence on the PZ demand of several key variables was assessed using ABAQUS. The slab effect was evaluated when the column and panel zone were provided with sufficient strength to remain elastic, and all plasticity occurred in the beams. Parameters were altered to assess their influence as described in Table 2. Reference model parameters from Table 1 are referred to below as ‘Ref’.

Table 2. *Elements modified to assess PZ demand.*

Group	Model ID	Element(s) Changed	Description
	ST-1	Slab Thickness (t_{ef})	130 mm
1	Ref	Slab Thickness (t_{ef})	150 mm
	ST-2	Slab Thickness (t_{ef})	170 mm
	BD-1	Beam Depth (d_b)	250 mm
2	Ref	Beam Depth (d_b)	298 mm
	BD-2	Beam Depth (d_b)	403 mm
	Ref	Slab Strength (f_c')	40 MPa
3	SS-1	Slab Strength (f_c')	50 MPa
	SS-2	Slab Strength (f_c')	60 MPa
4	TS-1	Slab Thickness (t_{ef}) & Slab Strength (f_c')	130 mm & 30 MPa

The PZ shear force demand depends on the external reaction forces of the subassembly, as illustrated in Figure 6. For an internal column in a bare steel frame (BSF), where both beams have the same moment capacity, the column shear force ($V^*_{C,BSF}$) can be expressed in Equation 8 where M_{pb} is the plastic moment capacity of the beams, L is the beam length, H is the column height, and L_c is the beam clear length.

$$V^*_{C,BSF} = \frac{2M_{pb}L}{HL_c} \tag{8}$$

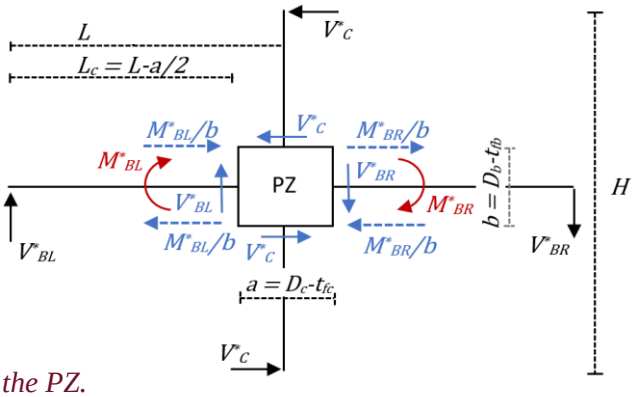

Figure 6. *Forces acting on the PZ.*

For an internal column, with two beams of the same size and a full depth slab (FDS) cast against the column, the column shear force ($V^*_{C,FDS}$) can be derived to be that in Equation 9, where M'_{pb} is the reduced beam plastic moment capacity accounting for axial interactions as per the Equations 1 to 3 as given in Equation 10 where N_s is the member axial capacity, and F_s is the slab peak bearing force on the column from Equation 1 but restated in Equation 11 for clarity. The panel zone demand increases proportionally to the column demand.

$$V^*_{C,FDS} = \frac{2M'_{pb}L}{HL_c} + \frac{F_sL}{2L_cH}(D_b + t_s) \tag{9}$$

$$M'_{pb} = min\left\{1.18M_{pb}\left(1 - \frac{F_s}{2N_s}\right); M_{pb}\right\} \tag{10}$$

$$F_s = min\{1.3t_{ef}b_{sef}(f'_c + 10MPa); 2N_s\} \tag{11}$$

Increases in column and PZ demand, assuming no column/PZ yielding, are given as $V^*_{C,FDS}/V^*_{C,BSF}$. This ratio is computed both (i) using the hand method with Equations 9 and 8, and (ii) from the detailed ABAQUS finite element analysis.

2.3.2 Capacity assessment

To observe the change in capacity of the PZ due to slab effects, the beams were made elastic, and the column and panel zone were permitted to yield. The panel zone strength was varied with different web doubler plate thickness to assess their influence on capacity as shown in Table 3.

***Table 3**. Elements modified to assess PZ capacity.*

Group	Model ID	Element(s) Changed	Description
	DB-1	Doubler Plate Thickness	0mm
	DB-2	Doubler Plate Thickness	2 x 4 mm
5	DB-3	Doubler Plate Thickness	2 x 8 mm
	Ref	Doubler Plate Thickness	2 x 16 mm
	DB-4	Doubler Plate Thickness	2 x 25 mm

Panel zone strength estimation directly from the finite element analysis is not straight forward. It is possible to obtain the peak column shear strength, together with the beam shears at this strength, and using standard equations for bare steel frames to obtain the panel zone shear strength. However, this was not considered to be accurate enough when a slab existed.

The increase in panel zone strength was assessed as follows.

1) Using the finite element software the displacement was applied to the top column node to obtain the column force versus subassembly drift.
2) At each subassembly drift,
    a. the panel zone deformations, Δ1 and Δ2 shown in Figure 7 were obtained.

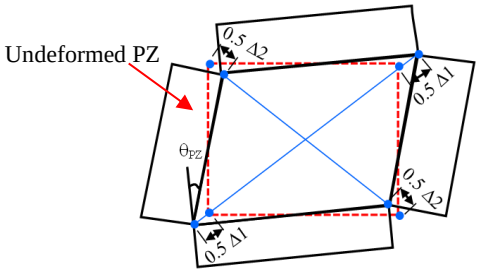

***Figure 7.** Deformed PZ measurements.*

b. The PZ shear deformation, θ_{PZ}, is computed by Equation 12 from Δ1 and Δ2 in Figure 7 (Civjan 1998) where *a* and *b* are the PZ dimensions given in Figure 6.

$$\theta_{PZ} = (\Delta 1 - \Delta 2)\frac{\sqrt{a^2+b^2}}{2ab} \tag{12}$$

c. The PZ contribution to subassembly displacement, Δ_{pz}, is then found using Equation 13 (Krawinkler et al. 1971) using the subassembly dimensions in Figure 6.

$$\Delta_{PZ} = \theta_{PZ} D_b - \left[\left(\frac{\theta_{PZ} L_b}{L_b + (0.5 D_c)}\right) H\right] \tag{13}$$

3) The panel zone deformation contribution, Δ_{pz}, is plotted against total subassembly drift as shown in Figure 8a. A line tangent to the post-yield linear portion of this curve was drawn.

4) The point at which this tangent line deviates from the curve gives the drift at which the panel zone has yielded completely as shown on Figure 8a.

5) By projecting vertically down to the x-axis, the subassembly drift at which the panel zone has completely yielded is then obtained.

6) Using Figure 8b, the column shear demand when the panel zone is yielding is found for the BSF and FDS subassemblies, V_{c_BSF} and V_{c_FDS}, respectively. V_{c_FDS}/V_{c_BSF} is greater than 1.0 indicates panel zone strength increase.

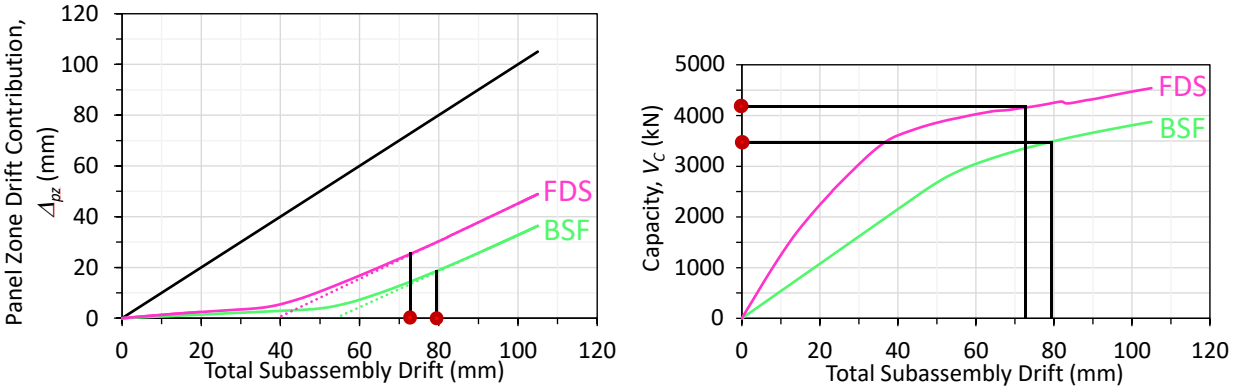

***(a)** Drift Contribution* ***(b)** Strength Estimation*

***Figure 8**. Schematic for PZ Strength estimation*

2.3.3 Mechanism Analyses

NZS3404 (2007) accounts for PZ strength increase from the slab by reducing design demands as described in Equations 5 and 6. It is more rational to consider the strength increase on the capacity, rather than on the demand side of the capacity-demand equation. A reason why the capacity may be increased is because the PZ yield mechanism differs from that of the original Krawinkler model shown in Figure 9a. It may be seen in Figure 9b that for deformations to be compatible with the slab, relocated, and extra plastic hinges are required to form a yield mechanism. To develop these hinges requires extra plastic work, and this results in a greater panel zone strength.

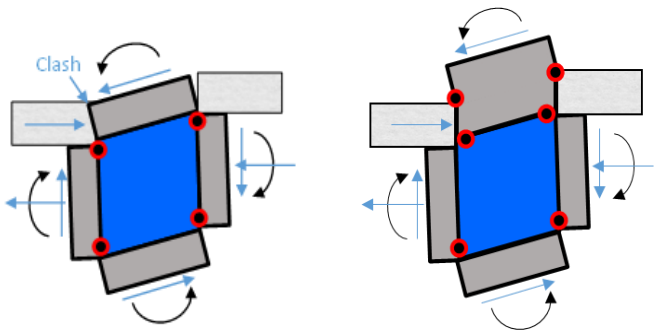

***a)** Incompatible* ***b)** Compatible*

***Figure 9.** Frame with slab plastic mechanism*

3 BEHAVIOUR

3.1 Slab Effect Upon Column Demands

For subassemblies elastic columns and PZs, and yielding beams, Figure 10a and 10b demonstrate that deeper slabs and beams increased the column, and hence PZ demand, confirming MacRae et al. (2007). Figure 10c shows that the slab compressive strength was relatively unimportant over the likely range. Full-depth slab models showed prominent peaks in strength as the concrete slab around the column reached its capacity before spalling thereby lowering the subassembly strength. It was only after spalling that Mode 2 became the governing force transfer mechanism. The bare steel frame (BSF) 403 mm deep beam model (BD-2), shown in Figure 10b, decreases in strength after yielding. This is because the section selected was slender causing significant buckling.

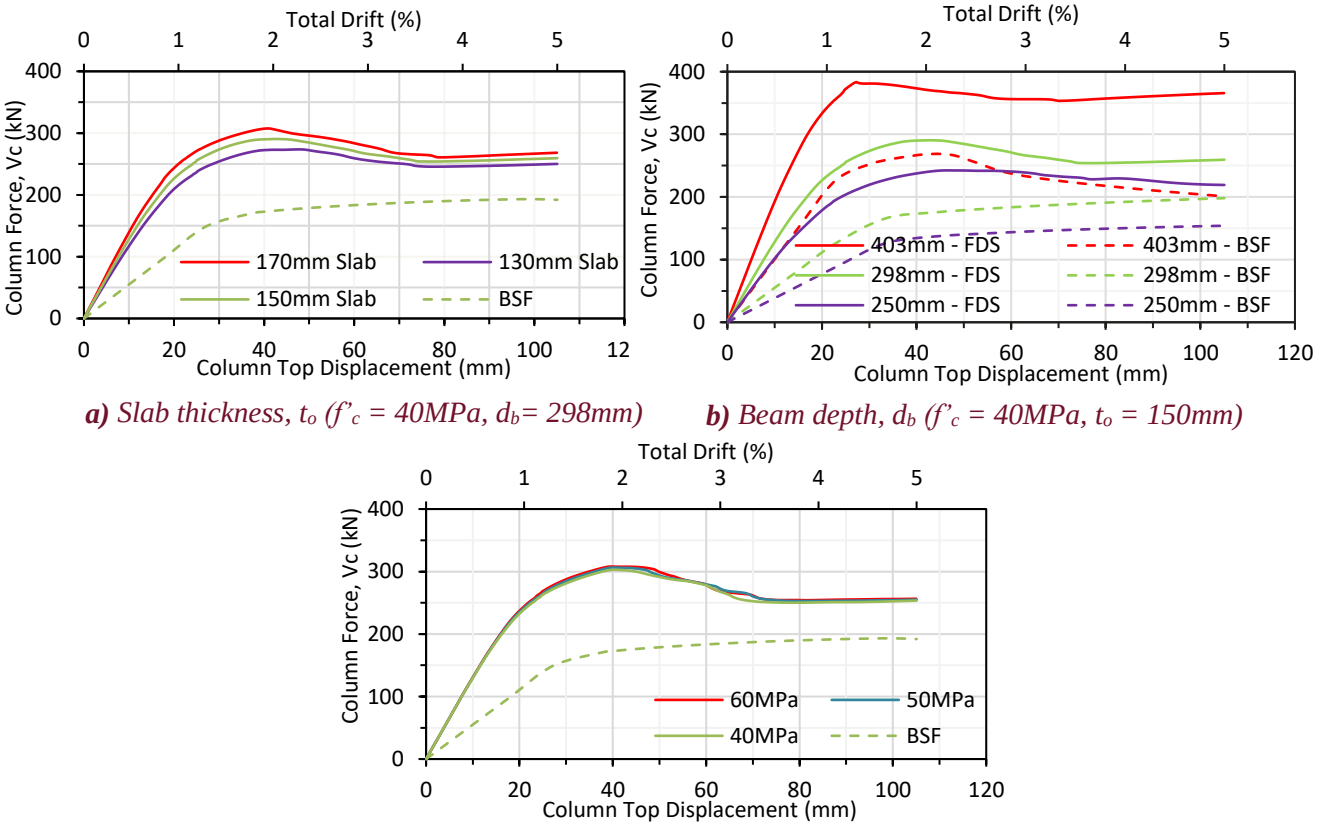

a) *Slab thickness, t_o (f'_c = 40MPa, d_b= 298mm)*

b) *Beam depth, d_b (f'_c = 40MPa, t_o = 150mm)*

c) *Concrete strength, f'_c (d_b = 298mm, t_o = 150mm)*

Figure 10. *Slab thickness, beam depth and concrete strength effects on subassembly strength*

The ratio between peak lateral force demand with and without a slab, $V^*_{C,FDS}/V^*_{C,BSF}$, was determined for each model, as shown in Table 4 for (i) the finite element (ABAQUS) model, and for (ii) the hand approach using Equations 9 and 8. The final column in the table shows that $V^*_{C,FDS}/V^*_{C,BSF}$ obtained from Equations 9 and 8 showed good agreement with the finite element analyses with a variation of less than 5% in most cases.

3.2 Slab Effect on Panel Zone Capacity

Figure 11a and 11b show the PZ drift contributions relative to the total subassembly drift for the BSF and FDS models respectively for the cases in Table 3. When there is a slab (i.e. FDS model), the PZ contribution to the total deformation increases because the beam becomes more stiff than it is in the bare steel (BSF) case.

***Table 4**. Demand increase ratios found for (i) ABAQUS and (ii) Equations.*

Model	(i) ABAQUS Demand Ratio	(ii) Equation 9 and 8 Ratio	[(ii)/(i) – 1]%
Ref	1.76	1.79	+1.7%
TS -1	1.61	1.53	-5.0%
ST-1	1.66	1.79	+7.8%
ST-2	1.86	1.90	+2.2%
BD-1	1.92	1.90	-1.0%
BD-2	1.70	1.64	-3.5%
SS-1	1.76	1.83	+4.0%
SS-2	1.77	1.83	+3.4%

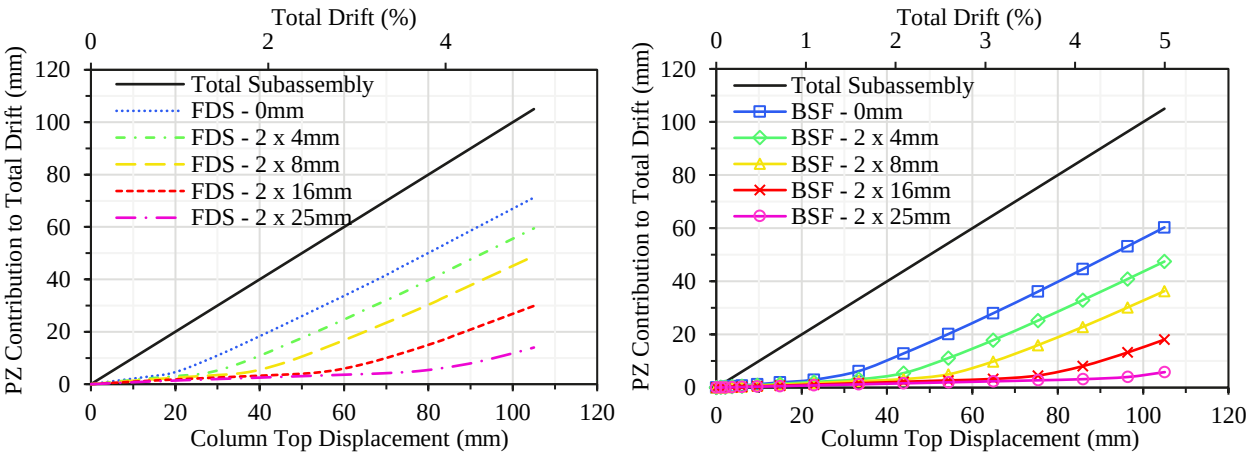

***(a)** FDS* *(b) BSF*

***Figure 11.** PZ drift contribution for different doubler plate thickness.*

The PZ capacity increases found using methods described in Section 2.3.2 are summarised in Table 5. The 2 x 25 mm doubler plate model (DB-4) is not shown as the model was strong and did not exhibit a complete mechanism at the drifts considered. The relative capacity increase ranged from 19% to 24%. For a typical beam depth of 400mm and slab depth of 150mm, the increase in overstrength factor demand due to the slab is about 40% according to Equation 5. Given that the strength is increased by 20%, the increased demand on the panel zone above it's strength is about 20%/40% = 50% of the increase in demand on the column. This ratio is consistent with the ratio of 0.54/1.08 = 50% from NZS3404 according to Equations 5 and 6.

***Table 5**. PZ capacity increase for models of varying strength.*

Model ID	Total Doubler Plate Thickness (mm)	Column Shear Force at PZ Yield (kN)		Capacity Increase (%)
		FDS (kN)	BSF (kN)	
DB-1	0	272	219	24
DB-2	8	352	284	24
DB-3	16	425	347	22
Ref	32	545	459	19

The reason for the strength increase can be attributed to a change in the yield mechanism of the PZ and the column. FE analyses in Figure 12 show the plastic hinge locations at large drifts. When the slab is present hinges form at the top of the slab as shown in Figure 12a. With no slab, they occur above the beam flanges as shown in Figure 12b. This is consistent with Figure 9.

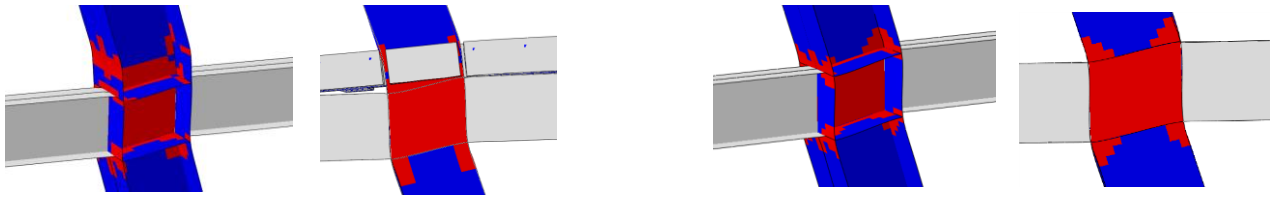

a) *FDS Mechanism (with slab)* ***b)*** *BSF Mechanism (without slab)*

Figure 12. *Physical change in mechanism obtained from ABAQUS. Yielding regions are shown in red.*

3.3 Design Recommendations

For design, it is considered rational if the demand increase and capacity increase are considered in the demand and capacity sides of the design approach respectively. This will increase the understanding and generality of the approach. Given the strength increase of the PZ due to the slab is 20% for the cases studied, and design equations accurately predict the demand increase, it is simply suggested that until better information is available the bare steel design capacity, V_{pz}, as predicted by Equation 7 should simply be multiplied by 1.2 as per Equation 14 to obtain the increased capacity with the slab, $V_{PZ,S}$.

$$V_{PZ,S} = 1.2V_{PZ} \tag{14}$$

In design the PZ capacity, $\phi V_{PZ,S}$, should be greater than the PZ demand, $V^*_{PZ,S}$, according to Equation 15 where $V^*_{PZ,S}$ is the PZ slab demand determined by Equation 16.

$$\phi V_{PZ,S} \geq V^*_{PZ,S} \tag{15}$$

$$V^*_{PZ,S} = \frac{\Sigma M'_{pb}}{d_b - t_{fb}} + F_s - V^*_{C,FDS} \tag{16}$$

By substituting in Equation 9, the above can be written as Equation 17 where M'_{pb} and F_s are found using Equation 10 and 11, respectively.

$$V^*_{PZ,S} = F_s\left(1 - \frac{L}{2L_cH}(D_b + t_s)\right) + 2M'_{pb}\left(\frac{1}{d_b - t_{fb}} - \frac{L}{HL_c}\right) \tag{17}$$

4 CONCLUSIONS

This study considered the validity of current NZS 3404 design methods for the panel zones in steel moment frames with concrete slabs. For the configurations considered, it is shown that:

1. The column, and panel zone, shear demand could be predicted well with simple equations.
2. The presence of a concrete slab increased the capacity of the PZ by approximately 20% for the cases considered due to a change in yield mechanism.
3. The increase in strength coupled with the increase in demand was approximately consistent with that in the current NZ standard where these effects are treated as a combined effect on the demand.
4. A rational method for panel zone design is proposed where the panel zone demand and capacity are considered explicitly.

5 REFERENCES

Alizadeh, S., Kosinanonth, K., MacRae, G. A., Webb, G., and Chaudhari, T. (2018). "Column Moment Demands from Orthogonal Beam Twisting." *Key engineering materials*, 763, 259-269.

American Institute of Steel Construction (2016). "Seismic Provisions for Structural Steel Buildings." Committee on Specification Chicago, Illinois.

Carson, W. (2023). "Best Practice, Specification, Detailing and Project Delivery [LECTURE]." ENCI436: Behaviour and Design of Structures. University of Canterbury.

Chaudhari T., MacRae G. A., Bull D., Clifton G. C. and Hicks S. J., " A Simple Mechanical Model for Steel Beam – Column Slab Subassembly Nonlinear Cyclic Behaviour", Journal of Earthquake Engineering. Published online: 02 Nov 2022. DOI:10.1080/13632469.2022.2139308

Civjan, S. A. (1998). "Investigation of retrofit techniques for seismic resistant steel moment connections." Doctor of Philosophy, The University of Texas, Austin.

European Committee for Standardization (1998). "Design of Structures for Earthquake Resistance - Part 1: General rules, seismic actions and rules for buildings ".

Henderson, C., Macalister, E., MacRae, G. Bashiri, M. (2023). "Panel Zone Strength in Moment Frames with Slabs." University of Canterbury, Christchurch, New Zealand.

Krawinkler, H. (1978). "Shear in Beam-Column Joints in Seismic Design of Steel Frames." *Engineering journal (New York)*, 15(3), 82-91.

Krawinkler, H., Bertero, V. V., and Popov, E. P. (1971). *Inelastic behaviour of steel beam-to-column subassemblages.*

MacRae, G., Clifton, G. C., and Mago, N. (2007). "Overstrength effects of slabs on demands on steel moment frames." 275-282.

MacRae, G., and Gunasekaran, U. (2007). "A concept for consideration of slab effects on building seismic performance." New Zealand Society for Earthquake Engineering.

Mago, N., and Clifton, C. (2008). "HERA REPORT R4-140: Investigation of the Slab Participation in Moment Resisting Steel Frames ". New Zealand Heavy Engineering Research Association, Manukau City, Auckland, New Zealand.

Simulia. (2022). ABAQUS. Dassault Systèmes.

Skiadopoulos, A., Elkady, A., and Lignos, D. G. (2021). "Proposed Panel Zone Model for Seismic Design of Steel Moment-Resisting Frames." *Journal of structural engineering (New York, N.Y.)*, 147(4).

Standards New Zealand (2007). "AS/NZS 3404: Steel Structures Standard". Published initially in 1997 with amendments.